

## **Dynamic Strain Measurement Using Improved Bonding Fiber Bragg Grating**

**Gwo-shyang HWANG, Chien-ching MA**

**Department of Mechanical Engineering, National Taiwan University**

**Taipei, Taiwan; E-mail: gshwang@ntu.edu.tw, ccma@ntu.edu.tw**

### **Abstract**

This study proposes an improved bonding method for attaching a fiber Bragg grating (FBG) on surface of a structure to measure its dynamic strains. The improved bonding fiber Bragg grating is called IBFBG for short in this study. The bonding method provides the chance to let the IBFBG and resistance strain gauge measure the longitudinal strain at the same point. This study use two steel cantilever beams, one with rectangular cross section and the other with circular, to demonstrate the ability of the IBFBG in dynamic strain measurements. Their dynamic strains are induced by impacts of a steel ball in free-fall transversely or in pendulum axially, respectively. The obtained strain time histories from both the IBFBG and strain gauge are nearly proportional in amplitudes; in addition, the Fourier spectra of those time histories show the IBFBG recognizes the natural frequencies of the cantilever beams up to 20000 Hz.

**Keywords:** Strain, Dynamic, Fiber Bragg Grating, Sensor

### **1. Introduction**

In recent years, for example, Perez et al. <sup>[1]</sup>, Betz et al. <sup>[2]</sup> and Tsuda et al. <sup>[3]</sup> have demonstrated the ability of FBG sensors on detection of acoustic emission signals and surface Lamb wave up to an order of 1.0 and 0.1 MHz, respectively. Therefore, the ability of FBG sensors in dynamic measurement is beyond doubt. However, the study for quality of its dynamic measurement is lack to date, except Measures et al. <sup>[4]</sup> has made a comparison between a resistance strain gauge and an FBG sensor up to 20 Hz. In the performance of resistance strain gauges, Harding and Welsh <sup>[5]</sup> has conduct refined impact tests for fibre-reinforced composites up to a strain rate 1000 sec<sup>-1</sup>, in which the strains from resistance strain gauges were confirmed through careful validations. That is equivalent to a simple harmonic strain vibration with amplitude of 0.25 in 1 kHz. Based on this, the ability of a resistance strain gauge is at least 1 kHz.

In previous studies, for example, <sup>[6]</sup>, the reflected spectra from the traditional bonding grating zone (with glue on the full grating zone) show multiple peaks with lower intensity at larger

strains due to sensitive responses to variations of strains in every point of the glued grating zone. This phenomenon results in difficulty to recognize the Bragg wavelength. To overcome this disadvantage, this study proposes an improved bonding method for an FBG sensor in which the glue is restricted to distribute on the two ends of its grating zone along the optic fiber, and the grating zone is free from the glue to retain its sensitivity on the average strain, over the grating zone.

This study devotes to the improved bonding FBG (IBFBG) sensor, and provides experimental results to show that the IBFBG sensor has the ability to measure the dynamic strain responses of a structure in the transient situation. In order to examine the dynamic measurement ability of the IBFBG, we compare its results with those obtained simultaneously from a resistance strain gauge.

## 2. Principle

Consider an IBFBG that is bonded on the tensile side of a bending specimen. Average strain,  $\Delta L/L$ , in the glue-free grating zone, e.g., between longitudinal distances  $x_1$  and  $x_2$  from the central line of span (with  $L=x_1-x_2$ ), is

$$\frac{\Delta L}{L} = \frac{1}{L} \int_{x_1}^{x_2} \varepsilon(x) dx = \frac{c}{L} \int_{x_1}^{x_2} \kappa(x) dx = \frac{1}{L} \frac{c}{EI} \int_{x_1}^{x_2} M(x) dx = \frac{c}{EI} \bar{M} \quad (1)$$

where  $x$ ,  $\kappa$ ,  $M$ , and  $I$ , are location, curvature, bending moment, and moment of inertia of a cross section, and  $E$  and  $c$  are Young's modulus of material and distance between neutral axis and fiber core, respectively. Therefore, a strain gauge to measure the average strain (over the grating zone) should be bonded with its center on a location, where the average bending moment  $\bar{M}$  occurs. In the situation of compressive side of bending, the IBFBG is shortened; although there is potential of larger compressive strain in the IBFBG than the structural surface, the difference in compressive strains between the IBFBG and the surface can be neglected except for the case of very large curvature.

A required pre-strain is needed for an IBFBG to retain the linear function between its axial strain and Bragg wavelength during axial tension and compression. The pre-strain is applied on an IBFBG in three steps: to bond only on one end of the grating zone and cure for a period of time, then applying tensile strain in the grating zone to a designated Bragg wavelength shift (corresponding to the required pre-strain), and to bond the other end.

### 3. Apparatus and Measurement Layout

Figure 1 shows the layout to carry out wavelength demodulation for the IBFBG. This study employed an FBG filter as a wavelength-to-amplitude converter <sup>[4,7]</sup>. The optic fiber is single mode (diameter 125  $\mu\text{m}$ ) manufactured by FIBERCORE, England. The strain gauge is the type KFG-1N-120-C1-11L2M2R, from KYOWA, Japan. The glue used for the IBFBG and strain gauge is cyanoacrylate instantaneous adhesive, type CC-33A, from KYOWA. The oscilloscope (WaveSurfer 64Xs, from LeCroy) with sampling rate of 2.5 MHz was used in this study.

Figures 2 and 3 show the rectangular and circular cantilever beam, respectively; in which the impact locations, and positions of the sensors are also shown. In particular, both sensors are located nearby in case of the rectangular beam, but located at the same location with strain gauge under the IBFBG in case of the circular beam. In order to produce transient bending or axial responses, this study used a free-fall steel ball or a pendulum (made of thread and a steel ball of diameter 12.7 mm) to impact on the cantilever beam transversely or on the free end cross section axially, respectively; in which transverse impacts of a free-fall steel ball was applied to both the beams, and axial impacts of the pendulum was only used for the circular beam. The free-fall steel balls for the rectangular and circular beam are of diameter 12.7 mm with fall distance 8.35 cm and of diameter 9.5 mm with fall distance 10.0 cm, respectively.

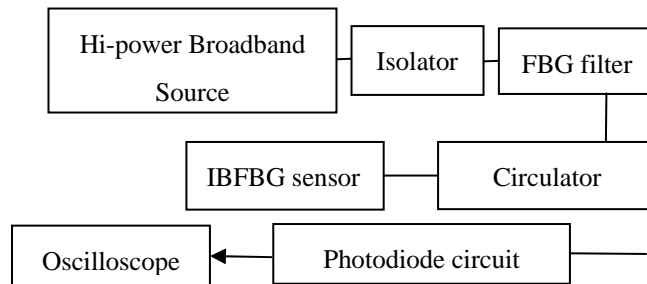


Figure 1. Wavelength demodulation for the IBFBG.

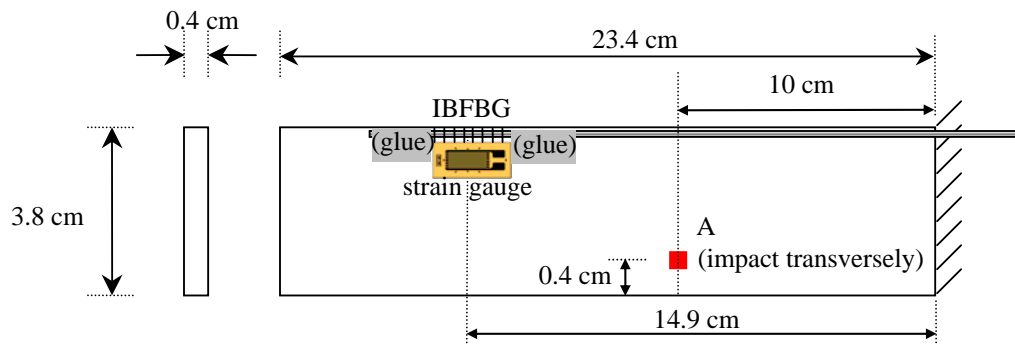


Figure 2. Rectangular cantilever beam used in this study, in which both sensors are located nearby.

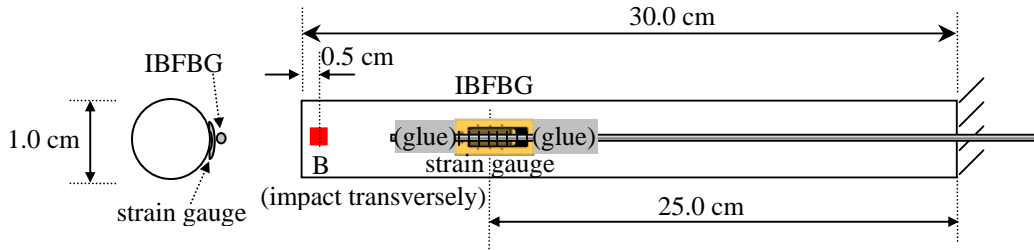


Figure 3. Circular cantilever beam used in this study, in which both sensors are located at the same position.

### 3. Experimental Results and Discussion

#### 3.1 Rectangular Cantilever Beam

As shown in Fig. 4, both the IBFBG and strain gauge attached nearby (Fig. 2) recorded the transient longitudinal strain responses in time span of 0.03 sec when the free-fall steel ball impacted at point A transversely (Fig. 2). In addition, its responses of intense fluctuation at the beginning of the first impact are zoomed in and shown in Fig. 5 in time span of 0.01 sec. Figures 4 and 5 clearly show that the highly proportionality between amplitudes of signals from both the sensors exists. This demonstrates that the IBFBG measures the average strain over the glue-free grating zone and similar to that obtained from the strain gauge. Figure 6 is the Fourier spectrum of the signals from the IBFBG; every peak inside presents one of the natural frequencies of the rectangular cantilever beam, including bending and torsional modes. Figure 6 also shows that the IBFBG discriminates natural frequencies up to 20000 Hz.

Furthermore, based on the Fourier spectra of signals from both the sensors, the amplitude ratios between the strain gauge and IBFBG show nearly constant for the initial three bending modes (under 1000 Hz); but for the torsional modes (larger than 700 Hz), the amplitude ratios is more lower than that for the initial three bending modes. This is the reason why in Figs. 4 and 5 some higher frequency amplitudes from the IBFBG are more evident than that from the strain gauge.

In this part, this study use the transient responses of the rectangular beam to compare the differences between the IBFBG and strain gauge, in which both the sensors attached near by. For rectangular beam, its torsional mode shapes will induce warping that varies in locations of both the sensors <sup>[8]</sup>, and it is difficult to carry out comparison and calibration using a strain gauge. Based on this, in the next part, this study used a circular beam to cancel the warping effects. In

addition, we also try to locate both the sensors on the same location to implement the possibility of calibration for the IBFBG using a common used strain gauge.

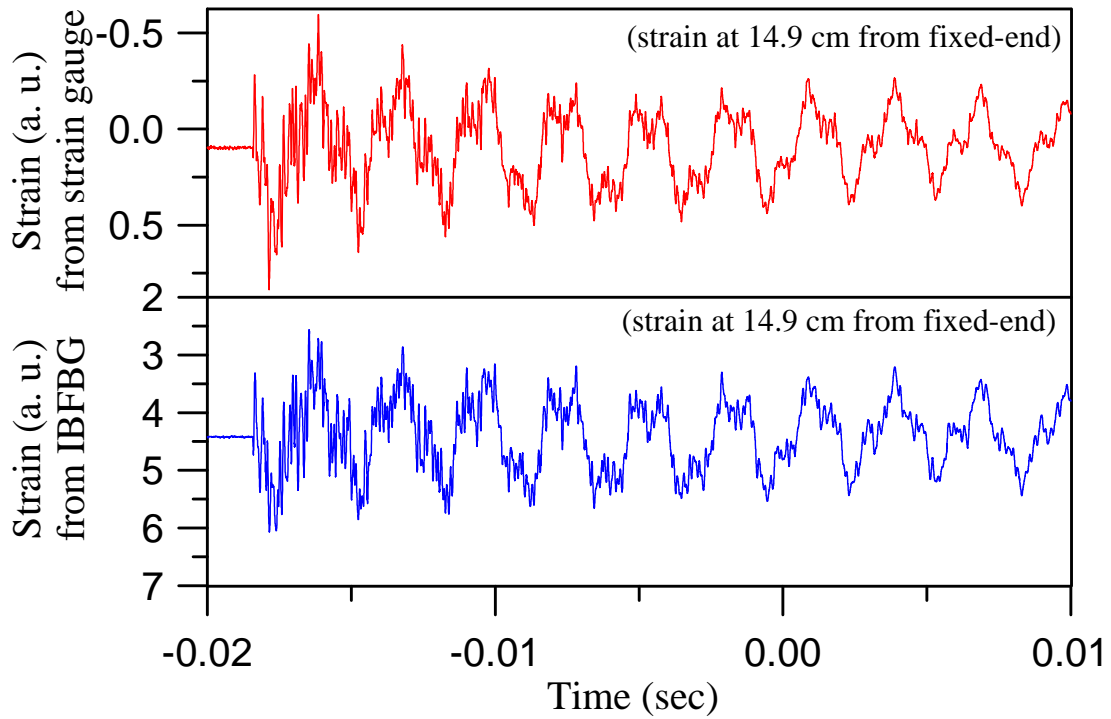


Figure 4. Transient strain responses of the rectangular beam from the IBFBG and strain gauge as free-fall steel ball impacted at point A (refer to Fig. 2).

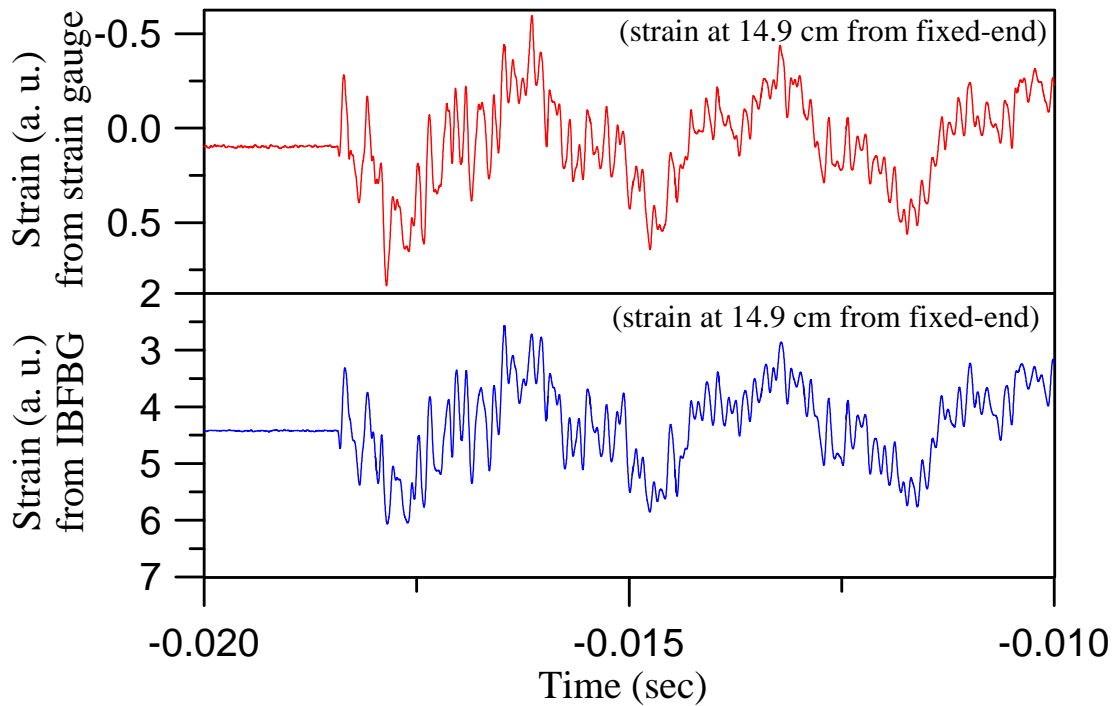


Figure 5. Zoom in of transient responses shown in Fig. 4 at the beginning of the first impact.

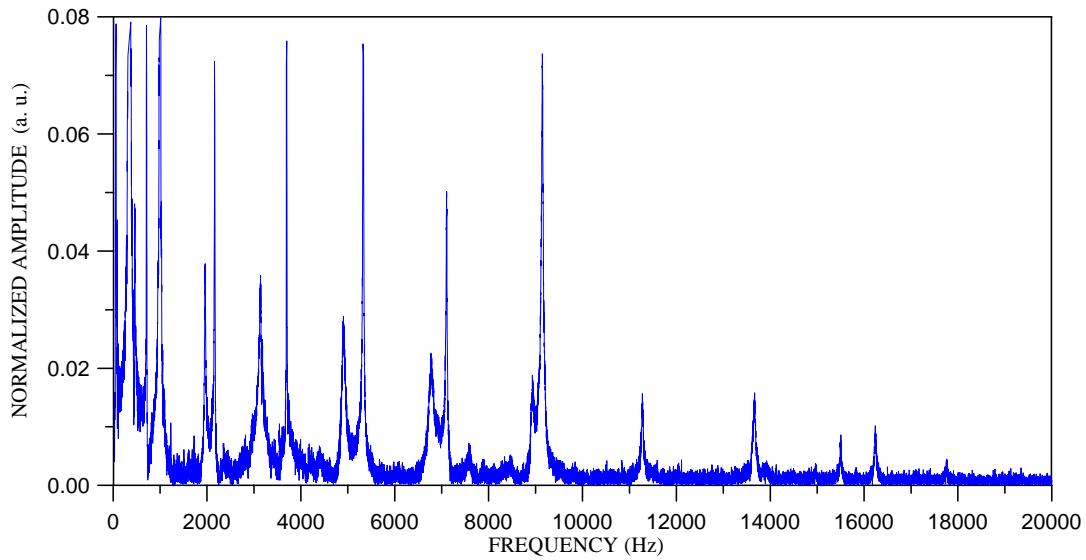


Figure 6. The Fourier spectrum of the signals from the IBFBG.

### 3.2 Circular Cantilever Beam

In Fig. 7, it shows axial pendulum impacted responses of the circular cantilever beam (Fig. 3); there are two impacts in 0.2 sec, the first impact at time of 0 sec and the second at time of 0.16 sec. Figure 8 presents the transient responses triggered by a transverse impact at point B (Fig. 3) in time span of 0.02 sec. In addition, Fig. 9 is the details in time span of about 0.004 sec for the signals in Fig. 8. In Fig. 9, the amplitudes of higher frequencies in signals from the strain gauge are more evident than those from the IBFBG. Based on the Fourier spectra of signals from both the IBFBG and strain gauge, the amplitude ratios between the strain gauge and IBFBG show nearly constant for the initial four bending mode shapes, under 3000 Hz, and lower amplitude ratios for other higher bending mode shapes. Such results can attribute to the influence of the strain gauge under the IBFBG (Fig. 3); the curvatures of the surface of strain gauge under are smaller than the curvatures of the structure surface, especially for those higher bending modes.

## 5. Conclusion

- (1) The improved bonding fiber Bragg grating (IBFBG) measures the average strain over the glue-free grating zone. It provides the chance to calibrate the signals of an FBG using a common used resistance strain gauge.
- (2) In this study, we used the rectangular and circular cantilever beam to compare the measures of both the IBFBG and strain gauge. The rectangular beam with both the

sensors attached nearby is not suitable for calibration due to the variation of warping effect between two locations of sensors. The circular beam with both the sensors attached at the same location shows that the curvatures of the surface of strain gauge under the IBFBG are smaller than the curvatures of the structure surface. In the near future, we will develop other method to calibrate an IBFBG.

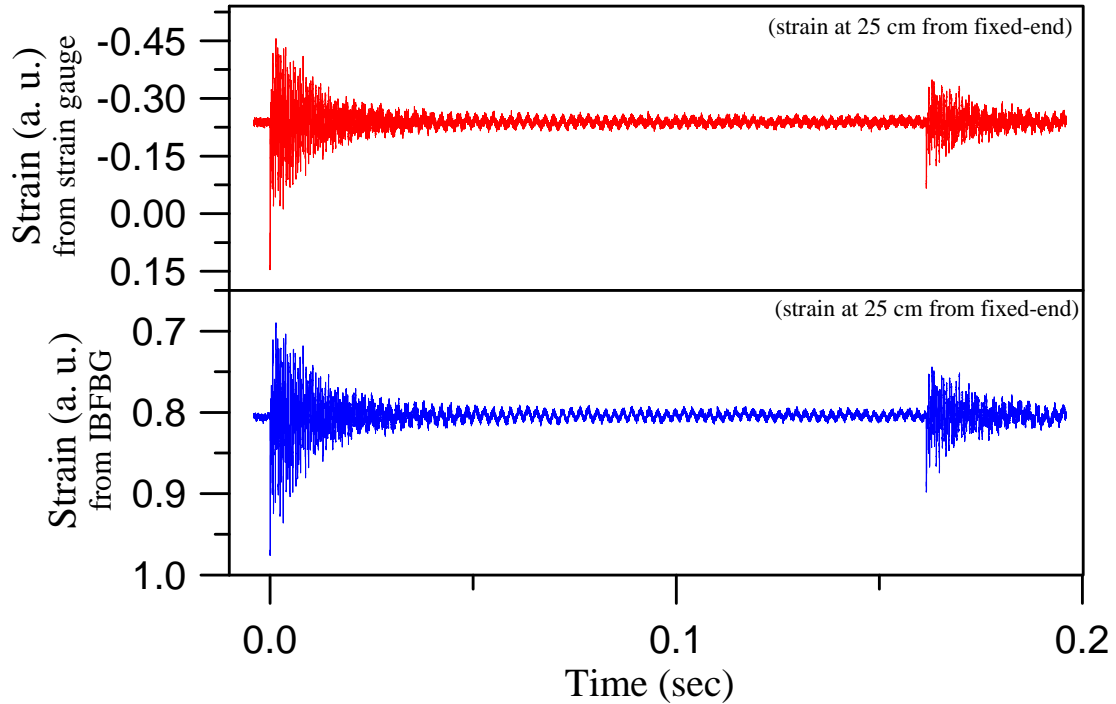


Figure 7. Axial pendulum impacted responses of the circular cantilever beam.

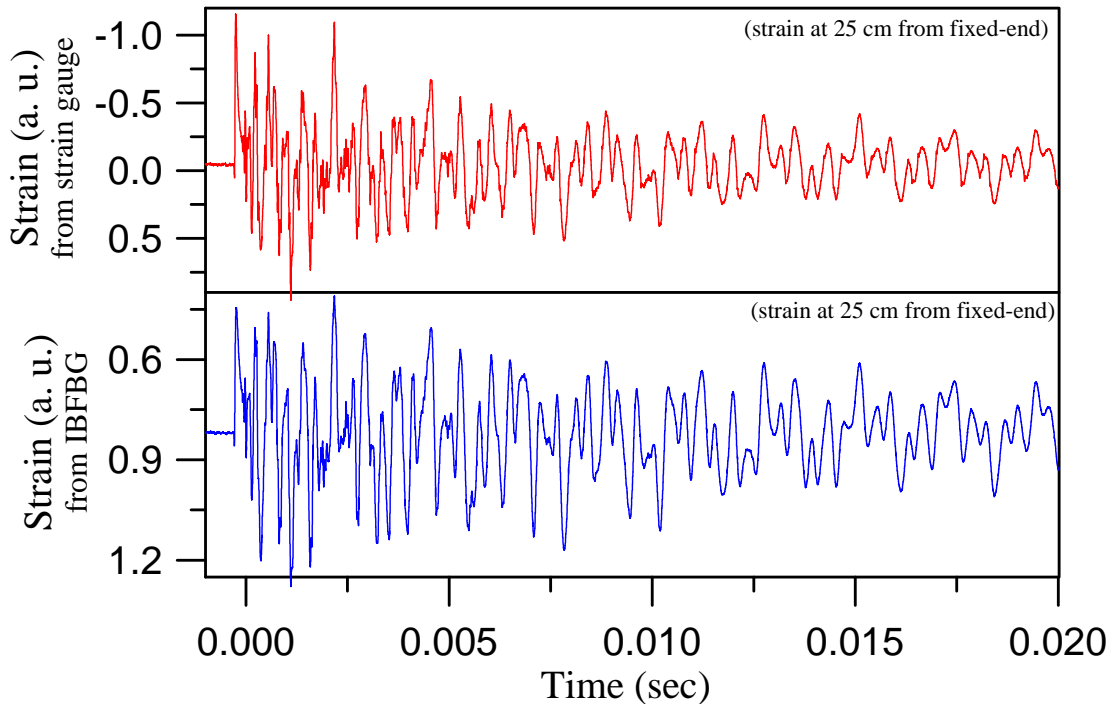


Figure 8. Transversely impacted responses of the circular cantilever beam.

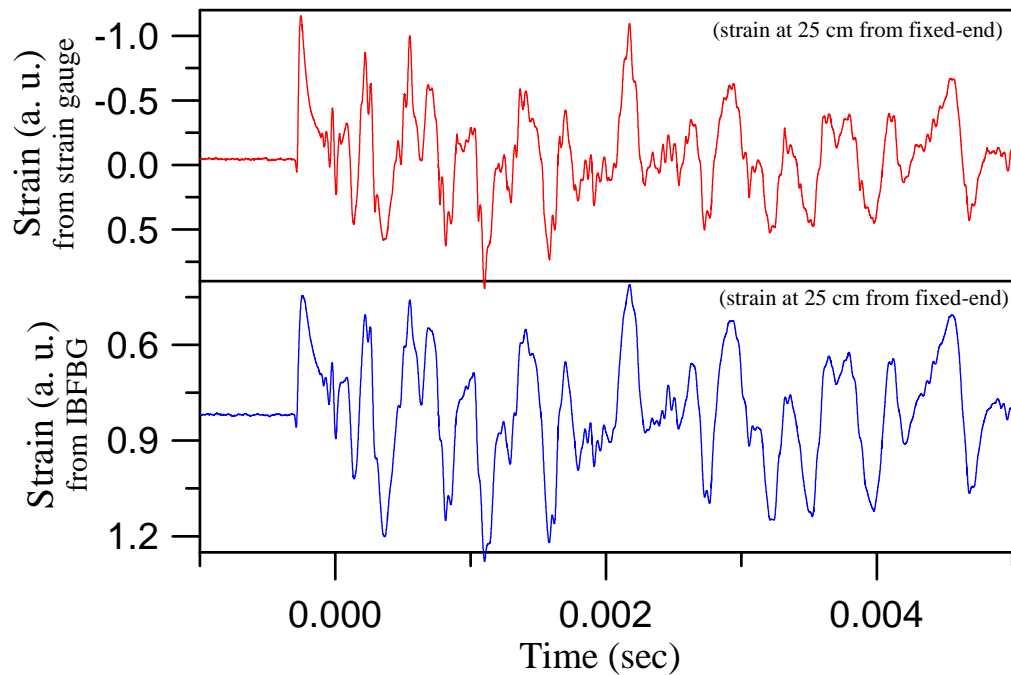


Figure 9. Details of the responses in Fig. 8.

## References

- [1] I. Perez, H. -L Cui, and E. Udd, "Acoustic emission detection using fiber Bragg grating," Proc. SPIE 4328, 2001, pp. 209-215.
- [2] D. C. Betz, G. Thursby, B. Culshaw, and W. J. Staszewski, "Acoustic-ultrasonic sensing using fiber Bragg gratings," Smart Mater. Struct. 12, 2003, pp. 122-128.
- [3] H. Tsuda, N. Toyama, K. Urabe, and J. Takatsubo, "Impact damage detection in CFRP using fiber Bragg gratings," Smart Mater. Struct. 13, 2004, pp. 719-724.
- [4] R. M. Measures, S. Melle, and K. Liu, "Wavelength demodulated Bragg grating fiber optic sensing systems for addressing smart structures critical issues," Smart. Mater. Struct. 1, 1992, pp. 36-44.
- [5] J. Harding, and L. M. Welsh, "A tensile testing technique for fibre-reinforced composites at impact rates of strain," J. Materials. Sci. 18, 1983, pp. 1810-1826.
- [6] H. -Y. Ling, K. -T. Lau, L. Cheng, and W. Jin, "Utilization of embedded optical fibre sensors for delamination characterization in composite laminates using a static strain method," Smart Mater. Struct. 14, 2005, pp. 1377-1386.
- [7] R. W. Fallon, L. Zhang, L. A. Everall, J. A. R. Williams, and I. Bennion, "All-fibre optical sensing system: Bragg grating sensor interrogated by a long-period grating," Meas. Sci. Technol. 9, 1998, pp. 1969-1973.
- [8] S. P. Timoshenko and J. N. Goodier, *Theory of Elasticity*. 3<sup>rd</sup> ed. New York: McGraw-Hill, 1970, pp. 309-313.